CrystEngComm

Accepted Manuscript

ROYAL SOCIETY OF CHEMISTRY

www.rsc.org/crystengcomm

Journal Name

ARTICLE

Power driven tunable white upconversion luminescence from the Lu_2TeO_6 tri-doped with Yb^{3+}, Tm^{3+} and Ho^{3+}

Received 00th January 20xx,
Accepted 00th January 20xx

DOI: 10.1039/x0xx00000x

www.rsc.org/

J. F. Tang,[a†] G. N. Li,[a] C. Yang,[a] J. Gou,[a] D. H. Luo,[a] and H. He[a]

Lu_2TeO_6 (LTO) doped with Yb^{3+}, Tm^{3+} and Ho^{3+} ions have been synthesized by the solid state reactions. Powder XRD and Rietveld refinement data confirmed that these compounds have a hexagonal structure with space group P321 (No. 150). The SEM images have shown the average size of the particles was smaller than 1 μm. Upconversion (UC) properties of the co-doped Yb,Tm:LTO and Yb,Ho:LTO as well as the tri-doped Yb,Tm,Ho:LTO were investigated under the excitation of 976 nm laser diode. The blue, green, and red UC emissions were realized and successfully combined to yield a white UC luminescence in the Yb,Tm,Ho:LTO. The light color were studied in the framework of 1931 CIE system. For the Yb,Tm,Ho:LTO, the UC light color can be continuously tuned in the white range by adjusting the pump power. Result has suggested that the Yb,Tm,Ho:LTO has a potential as phosphor for UC based white lighting and optoelectronic devices.

Introduction

The rare earth doped upconversion (UC) materials have attracted considerable interest owing to the potential applications in lighting, flat panel display, optoelectronic devices, and nano-biotechnology[1-5]. Many rare earth ions such as Er^{3+}, Tm^{3+}, and Ho^{3+} are used as light emitters because their abundant ladder-like energy levels are very convenient for metastable energy storage and realizing the conversion of near infrared (NIR) light to visible light. In most of the UC materials the Yb^{3+} ion is usually co-doped as sensitizer owing to its strong absorption around 980 nm. The UC luminescence can be enhanced through effective energy transfer processes[6, 7]. The Yb^{3+}, Tm^{3+}, and Ho^{3+} tri-doped systems are especially interesting because they can generate white light emissions[8-10].

Generally, the host matrix for UC luminescence should possess relatively low phonon energy to avoid efficiency losses via nonradiative transfer and should be comparable size to the trivalent rare earth ions doping. The most representative of these materials are the rare earth fluorides such as the LaF_3, $NaYF_4$, and $NaLuF_4$[11-13]. However, these materials suffered from relatively hash conditions for preparation and low chemical stability[14]. The complex oxide of rare earth hexaoxotellurates (Re_2TeO_6) have superior physical and chemical properties as well as relatively low phonon energy about 700 cm^{-1}, the distinguished characteristics make these compounds promising new materials for photo-electronic applications[15].

Some researchers have concerned the crystal structure of Re_2TeO_6. The studies have shown when Re = Y, La, Sm, and Gd the crystal structures are all belong to the orthorhombic crystal system (space group $P2_12_12_1$, No.19)[15-17]. The Lu_2TeO_6, although with a similar chemical composition, is of a different crystalline system (hexagonal, PDF#41-0138). Up to now only a few works on the Re_2TeO_6 as host matrixes for rare earth luminescent materials have been reported such as the Eu^{3+}:La_2TeO_6 [18] and Tb^{3+}:Gd_2TeO_6 [19]. The Lu_2TeO_6 doped with Eu^{3+} for luminescent material was firstly reported by S. Natansohn at 1969[20]. However, little or no attention has been dedicated to the study of rare earth oxytellurides as upconversion materials.

This work is devoted to the investigation of UC luminescence of Lu_2TeO_6 doped with Yb^{3+}, Tm^{3+}, and Ho^{3+} ions. The crystal structure parameters of the compounds have been refined. Under the excitation of 976 nm laser, the UC emissions were observed and the power driven white light tunability was firstly reported in the material. Result shows the Yb^{3+}, Tm^{3+}, and Ho^{3+} tri-doped Lu_2TeO_6 is potential for an application as phosphor in white lighting and optoelectronic devices.

Experimental

The compounds of Lu_2TeO_6 (hereafter LTO), Yb,Tm:LTO (5 at.% Yb^{3+} and 1 at.% Tm^{3+}), Yb,Ho:LTO (5 at.% Yb^{3+} and 1 at.% Ho^{3+}), and Yb,Tm,Ho:LTO (5 at.% Yb^{3+}, 2 at.% Tm^{3+}, and 1 at.% Ho^{3+}) were synthesized by a typical high temperature solid state reaction method. The starting chemicals of TeO_2 (purity 99.99%) and rare earth oxides Lu_2O_3 (purity 99.99%), Yb_2O_3 (purity 99.99%), Tm_2O_3 (purity 99.99%), and Ho_2O_3 (purity 99.95%) were accurately weighted according to their

[a] Faculty of Materials and Energy, Southwest University, Chongqing, 400715, China.
† To whom correspondence should be addressed. Tel: +86 023-6825-3204; Fax: +86 023-6825-3204; Email address: tangjf@swu.edu.cn.
Electronic Supplementary Information (ESI) available: [details of any supplementary information available should be included here]. See DOI: 10.1039/x0xx00000x

stoichiometric amounts. The raw materials were ground together thoroughly and pressed into tablets, then were firstly sintered at 750 °C in an alumina crucible for 10 hours. Next, the compounds were reground and secondly sintered at 900 °C for 12 hours in air. The finely ground polycrystalline compounds were obtained for measurements. The crystal structure of the as-prepared compounds were analyzed by a Shimadzu XRD-6100 X-ray diffractmeter with Cu-Kα radiation (λ = 0.15406 nm). The morphology images were taken by using a JEOL JSM-6510LV scanning electron microscope (SEM). The spectra of UC luminescence were measured by means of a PerkinElmer LS-55 luminescence spectrometer equipped with a laser diode (LD) centered at 976 nm as the pump source. The spectra were corrected taking the spectral sensitivity of the device into account. The incident pump power was measured by a Coherent FieldMax Ⅱ-TO power meter equipped with a PM10 thermopile sensor. All the spectral experiments were carried out at room temperature.

Results and discussion

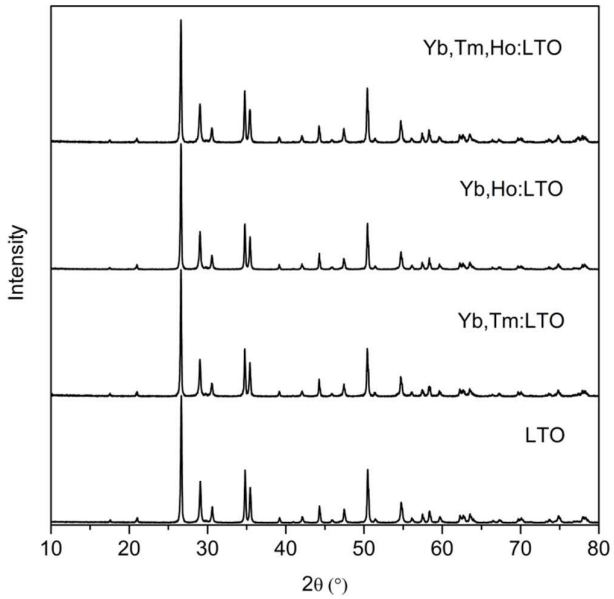

Figure 1. Powder XRD patterns of the as-prepared compounds.

Figure 1 shows the powder XRD patterns of the as-prepared compounds. By the doping of rare earth ions, no significant changes in the XRD patterns were observed and all diffraction peaks are matching well with the JCPDS File PDF#41-0138. This suggests that all the rare earth dopants have substituted the Lu^{3+} ions in the crystals. In order to further obtain the structural parameters of these compounds, a typical structural refinement by the Rietveld method was performed by using the Jana program[21]. The refinement results revealed that all the compounds crystallized in the hexagonal structure with space group P321 (No. 150). Figure 2 shows the observed, calculated and the difference XRD patterns of the LTO as a representative. The quality of structural refinement data was checked by the parameter of GoF (goodness of fit), which was found to be 1.40 (R_{wp}=17.88) for the LTO refinement. For perfect refinement the value of GoF should approach unity. In the present case the result has indicated a good agreement between the observed and calculated XRD patterns. The lattice parameters of the LTO were refined to be $a = b$ = 8.933(1) Å, c = 5.0674(5) Å, $\alpha = \beta$ = 90°, and γ = 120° with the formula units per cell Z = 3. The lattice parameters of all the compounds were listed in Table 1 for comparison. It can be seen that, the lattice parameters increase after the Lu^{3+} ions replaced by the rare earth ions of Yb^{3+}, Tm^{3+}, and Ho^{3+}. This could be interpreted as a direct result of the lanthanide shrinking effect.

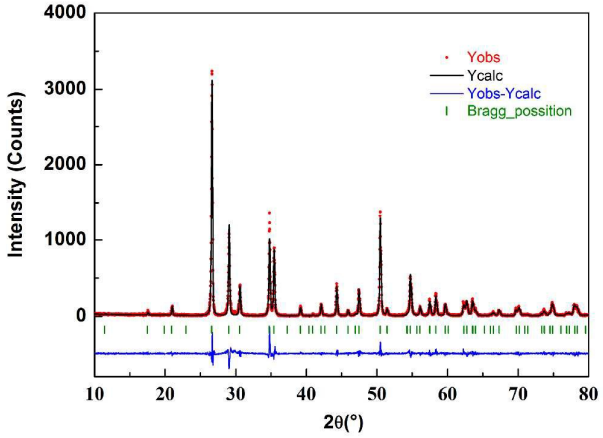

Figure 2. Observed, calculated and the difference XRD patterns for the Rietveld refinement of the LTO.

Table 1. Lattice parameters of the compounds after Rietveld refinement.

Compound	LTO	Yb,Tm:LTO	Yb,Ho:LTO	Yb,Tm,Ho:LTO
a (Å)	8.933(1)	8.942(1)	8.944(2)	8.9414(5)
b (Å)	8.933(1)	8.942(1)	8.944(2)	8.9414(5)
c (Å)	5.0674(5)	5.0718(9)	5.0724(9)	5.0721(3)
α, β, γ (°)	90,90, 120	90, 90, 120	90, 90, 120	90, 90, 120

Table 2. Rietveld refined atomic parameters of the LTO.

Atom	Wyckoff position	Site symmetry	Coordinates (x, y, z)		
Lu1	3e	C_2	0.6222(4)	0	0
Lu2	3f	C_2	0.2840(4)	0	0.5
Te1	1a	D_3	0	0	0
Te2	2d	C_3	0.3333	0.6667	0.509(4)
O1	6g	–	0.074(6)	0.864(5)	0.770(5)
O2	6g	–	0.434(5)	0.582(6)	0.727(6)
O3	6g	–	0.211(4)	0.755(5)	0.258(5)

Table 2 lists the refined atomic parameters of the LTO. Figure 3 illustrates the unit cell and layered graphs which were modeled according to the atomic parameters by using the Diamond software[22]. In the LTO structure, both the Te(VI) and Lu(III) are coordinated six-fold by oxygen. This leads to an

octahedral oxygen coordination environment for the both cationic sites. The Te sites were distributed over two Wyckoff positions of the 1a with site symmetry of D_3 and the 2d with site symmetry of C_3. The Lu ions are located at the 3e and 3f Wyckoff positions and both of which have the same site symmetry of C_2. It can be expected that the rare earth ion doped in the LTO structure will be in a very different crystallographic environment by comparing with the cases in the orthorhombic compounds of Ln_2TeO_6 (Ln=Y, La, Sm, Gd), in which the rare earth ions occupy two independent cationic sites with the site symmetry of C_1 and are coordinated seven-fold by oxygen[23].

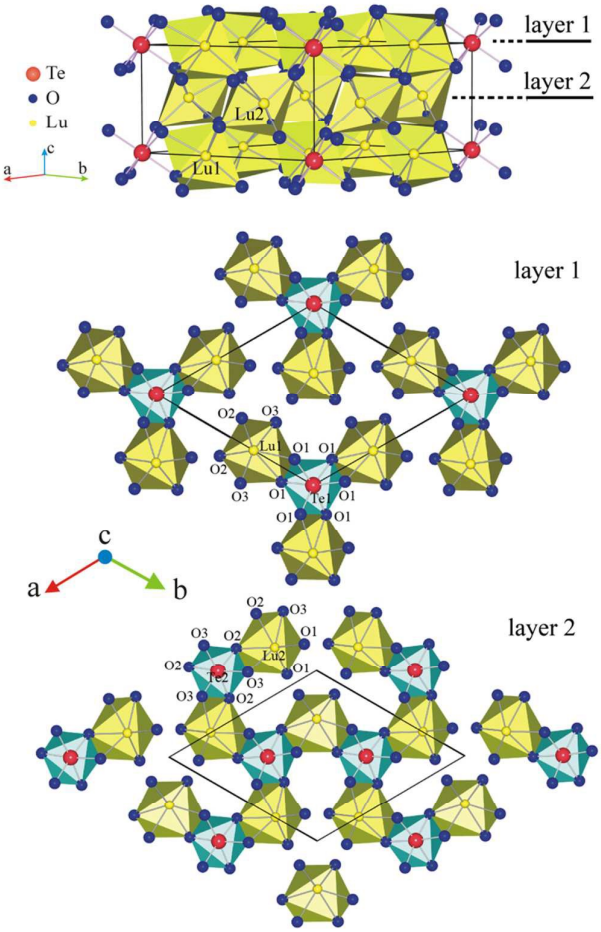

Figure 3. Schematic representation of the unit cell and layered graphs for the LTO.

Figure 4 shows the SEM images of the as-prepared compounds. It is clearly seen that the morphology of the particles are very similar for all the samples. The size distribution of the particles is not very uniform and it depends on the status of the starting materials, the reaction conditions, and also the grinding process. The average particle size is estimated smaller than 1 μm for all the samples.

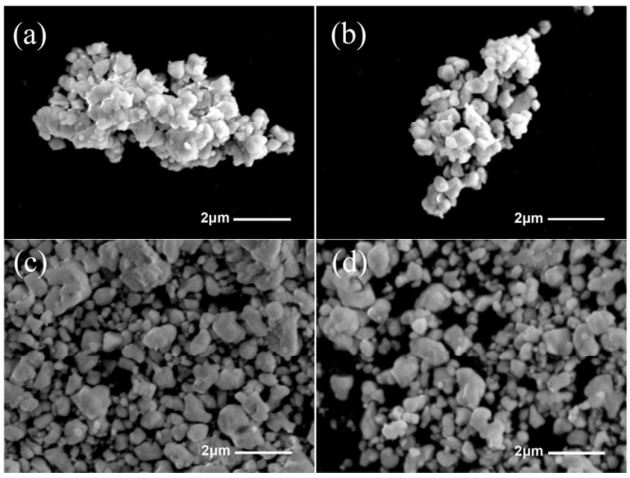

Figure 4. SEM images of the as-prepared LTO (a); Yb,Tm:LTO (b); Yb,Ho:LTO (c); and Yb,Tm,Ho:LTO (d) compounds.

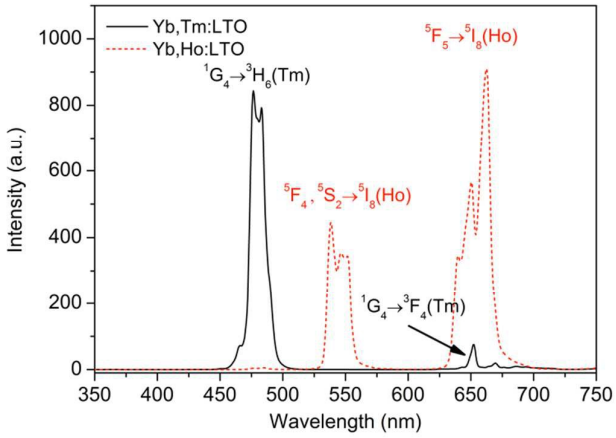

Figure 5. UC luminescence spectra of the Yb,Tm:LTO and Yb,Ho:LTO under the 976 nm excitation.

Figure 5 shows the UC luminescence spectra of the Yb,Tm:LTO and Yb,Ho:LTO under the 976 nm excitation with the same pump power. For the Yb,Tm:LTO there are two emission bands from the Tm^{3+} ions were recorded in the visible range. The strong blue band at around 475 nm can be assigned to the $^1G_4 \rightarrow {}^3H_6$ transition and the weaker red band at around 650 nm can be assigned to the $^1G_4 \rightarrow {}^3F_4$ transition. Two emission bands from the Ho^{3+} ions were also recorded for the Yb,Ho:LTO in the visible range. One is the green band at around 550 nm, which can be assigned to the $^5F_4, {}^5S_2 \rightarrow {}^5I_8$ transition and the other is the red band which can be assigned to the $^5F_5 \rightarrow {}^5I_8$ transition. It can be seen that the two red bands of Ho^{3+} and Tm^{3+} ions are both located at the same wavelength range, but the emission intensity of Ho^{3+} ions is much stronger than that of the Tm^{3+} ions.

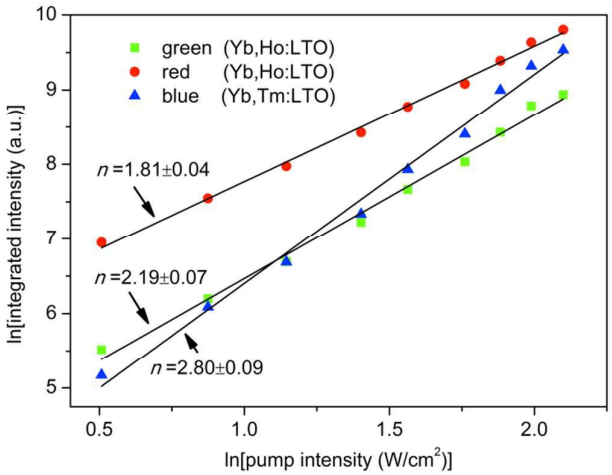

Figure 6. Pump intensity dependence of UC luminescence of the Yb,Tm:LTO and Yb,Ho:LTO, the value of *n* denote the fitted slope in double natural logarithmic scale.

The dependence of UC luminescence intensity on the pump power is essential to investigating the UC mechanism. For an unsaturated UC process, the integrated intensity of an UC emission band I_{UC} can be presented by[24]

$$I_{UC} \propto I_P^{\,n} \quad (1)$$

where I_P is the pump intensity and *n* is the number of photons involved in the process to populate the UC terminating level. The integrated UC intensities for the blue emission of the Yb,Tm:LTO and for the green and red emissions of the Yb,Ho:LTO versus the pump intensity are plotted in a double natural logarithmic scale in Figure 6. The fitted slope (*n*) is 2.80 for the blue emission of Yb,Tm:LTO, and 2.19 and 1.81 for the green and red emissions of Yb,Ho:LTO, respectively. It indicates that a three-photon process is necessary to produce the blue UC emission of Tm^{3+} while the both green and red UC emissions of Ho^{3+} should be ascribed to a two-photon process. The similar results have been discussed in the other systems such as the Y_2O_3[25], $NaYF_4$[26], and $BaYF_5$[27]. Furthermore, comparing with the two-photon green and red UCs for the Yb,Ho:LTO, the slope of the green UC is slightly greater than that of the red UC, it implies that the green UC would be more sensitive to the change of pump power. Figure 7 shows the UC spectra of the Yb,Ho:LTO normalized to the $^5F_5 \rightarrow {}^5I_8$ transition. The pump intensity was estimated as the pump power divided by the fluorescence spot area. The ratio of integrated intensities of green over red (GR ratio) at different pump intensities were evaluated and displayed in the inset of Figure 7. The GR ratio has maintained a nice growth trend with the pump intensity increase until it suffers a saturation when the pump intensity increased as high as ~9 W/cm^2. Possible reason for this interesting behavior will be analyzed closely following the next discussion about the UC mechanism.

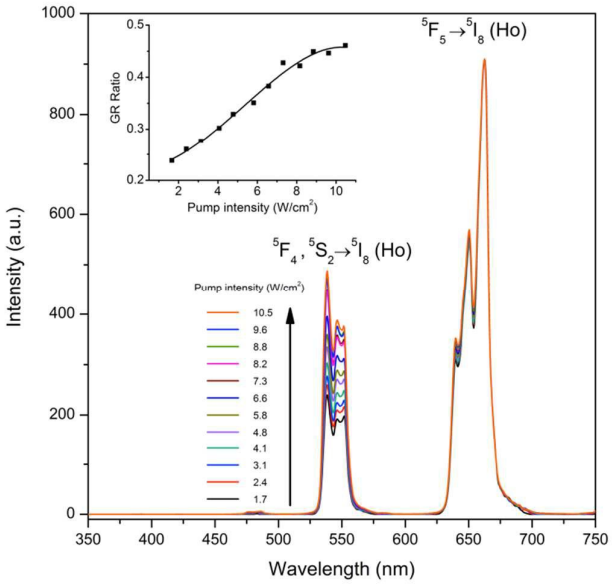

Figure 7. Pump intensity dependence of UC spectra for the Yb,Ho:LTO. The emission intensities are normalized to the $^5F_5 \rightarrow {}^5I_8$ transition in order to emphasize the evolution of the green UC. The inset shows the saturation behavior of the GR ratio.

Figure 8 shows the energy level diagrams of Yb^{3+}, Tm^{3+} and Ho^{3+} as well as the UC mechanisms corresponding to the blue, green, and red emissions. It can be seen that both the Tm^{3+} and Ho^{3+} ions have no energy level at the excitation of 976 nm. For the Yb,Tm:LTO, pumped by 976 nm laser the Yb^{3+} ions were excited from the ground state of $^2F_{7/2}$ to the $^2F_{5/2}$ level. Subsequently the energy transfer occurred between the $Yb^{3+}(^2F_{5/2})$ and $Tm^{3+}(^3H_6)$ ions. The $Yb^{3+}(^2F_{5/2})$ ions transferred the excitation energy to the $Tm^{3+}(^3H_6)$ ions, which made an effective population on the excited $^3H_5$ level of Tm^{3+} ions. Then the unstable $Tm^{3+}(^3H_5)$ ions would nonradiatively relax to the $^3F_4$ level immediately. Once again, the excited $Yb^{3+}(^2F_{5/2})$ ions would transfer their energy to pump the Tm^{3+} ions from the $^3F_4$ level to the $^3F_{2,3}$ levels. The Tm^{3+} ions in the $^3F_{2,3}$ levels would nonradiatively relax to the $^3H_4$ level. And then, the $Yb^{3+}(^2F_{5/2})$ ions thirdly transferred their energy to pump the Tm^{3+} ions from the $^3H_4$ level to the $^1G_4$ level. Finally, the excited $Tm^{3+}(^1G_4)$ ions relaxed to the ground state of $^3H_6$, by producing the blue emission at around 475 nm. Simultaneously a small portion of the excited $Tm^{3+}(^1G_4)$ ions relaxed to the $^3F_4$ level by producing the red emission at around 650 nm. The UC process in Yb,Ho:LTO could be discussed similarly to our previously reported Yb,Ho:NaLa$(MoO_4)_2$ system[28]. In the case of Yb,Ho:LTO, The $Yb^{3+}(^2F_{5/2})$ ions transferred the excitation energy to the $Ho^{3+}(^5I_8)$ ions and make the Ho^{3+} ions populate on the $^5I_6$ and $^5I_7$ levels. Then by the aid of energy transfer from the excited $Yb^{3+}(^2F_{5/2})$ ions once again or through excited state absorption (ESA) the $^5F_4$,$^5S_2$ and $^5F_5$ levels of Ho^{3+} could be populated effectively. Finally the green and red UC luminescence were generated through the transitions of $^5F_4$,$^5S_2$

$\rightarrow$ $^5I_8$ and $^5F_5 \rightarrow {}^5I_8$, respectively. Some multiphonon relaxations should play important roles in the both Yb,Tm and Yb,Ho systems and are illustrated in solid wavy lines with arrows in Figure 8. It also should be noted that, the energy transfer process in the Yb,Tm,Ho tri-doped system would be expectably more complicated than that in the co-doped systems. It is quite possible that, especially for the high Tm^{3+} concentration case, the energy transfer between the Tm^{3+} and Ho^{3+} ($^1G_4+{}^5I_8 \rightarrow {}^3H_6 + {}^5F_3$) would make the Tm^{3+} ions act as sensitizer for the UC of Ho^{3+} ions and further enhance the emissions of Ho^{3+} ions in a certain degree.

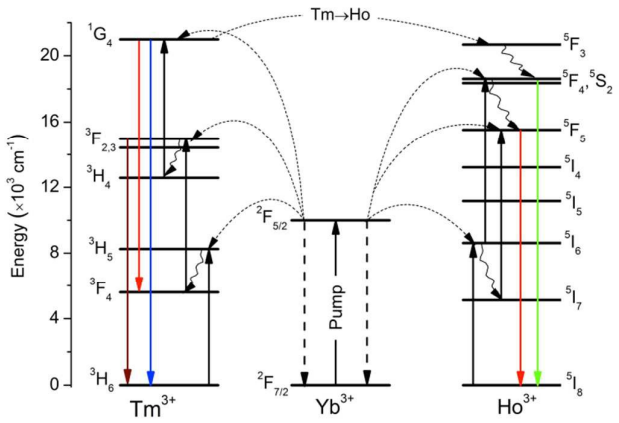

Figure 8. Energy level diagrams and schematic representation of the mechanisms responsible for the generation of UC luminescence for the Yb,Tm and Yb, Ho systems.

As mentioned earlier, in the Yb,Ho:LTO the GR ratio has exhibited a saturation behavior when the pump intensity is high enough (see the inset of Figure 7). This could be attributed to the saturation of the excited states of Ho^{3+}. Generally, the first excited level of $^5I_7$ would exhibit a much longer lifetime than the second excited level of $^5I_6$[29]. Under the strong excitation the Ho^{3+} ions will be fast and effectively populated on the $^5I_7$ level through the sequential processes of energy transfer ($^5F_{5/2}+{}^5I_8 \rightarrow {}^5F_{7/2}+{}^5I_6$) and multiphonon relaxation ($^5I_6 \rightarrow {}^5I_7$). Under such circumstances the population on the $^5I_7$ level will quickly reach saturation when suffered a strong excitation. This will directly lead to the red UC emission ($^5F_5 \rightarrow {}^5I_8$) hit a bottleneck because the red UC is realized mostly depend on the up transition of $^5I_7 \rightarrow {}^5F_5$. On the other hand, the population on the $^5I_6$ level has not yet reached saturation at the very moment. The green emission ($^5F_4/{}^5S_2 \rightarrow {}^5I_8$) which mostly depends on the up transition of $^5I_6 \rightarrow {}^5F_4/{}^5S_2$ will continue to grow fast until the $^5I_6$ level also reach saturation at the stronger pump intensity. When the populations on the $^5I_7$ and $^5I_6$ levels both reach saturation at certain pump intensity (> ~9 W/cm^2), the GR ratio will remain almostly unchanged with the pump power further increased.

The Yb,Tm and Yb,Ho in LTO host matrix have characterized very interesting UC properties. Based on the emissions of the Yb,Tm:LTO and Yb,Ho:LTO, it is expectable to produce UC white emission by appropriate tri-doping of Yb^{3+}, Tm^{3+}, and Ho^{3+} in LTO compound. Figure 9 shows the UC luminescence spectra of the Yb,Tm,Ho:LTO under the 976 nm laser excitation with different pump intensities. Compared to the spectra of the binary dopant systems, it is easy to assign the origin of all the emission bands in the tri-doped system except for the emission band around 700 nm, which can be assigned to the transition $^3F_{2,3} \rightarrow {}^3H_6$ of Tm^{3+} according to the energy level diagrams. It can be found that with the increase of pump intensity, the blue emission of Tm^{3+} was enhanced more significantly than the green and red emissions of Ho^{3+}.

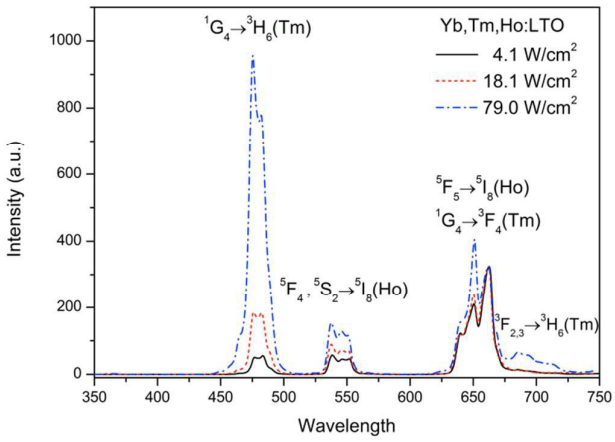

Figure 9. UC luminescence spectra of the Yb,Tm,Ho:LTO under 976 nm laser excitation.

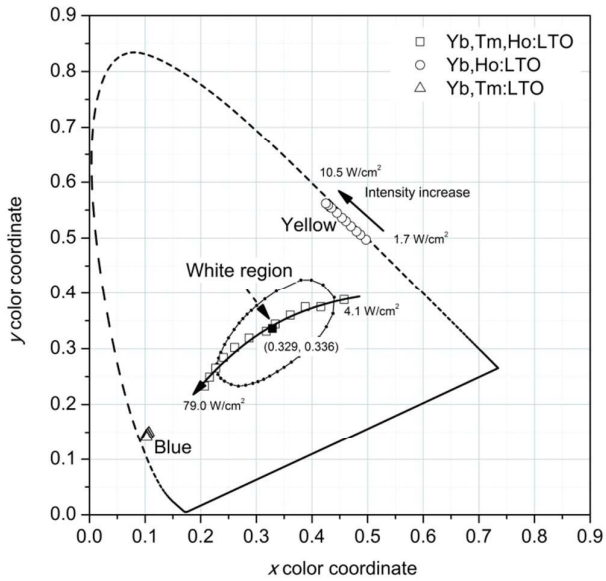

Figure 10. The calculated color coordinates in a 1931 CIE chromaticity diagram.

The color coordinates of the Yb,Tm,Ho:LTO as well as the co-doped Yb,Tm:LTO and Yb,Ho:LTO were calculated according to the spectra and depicted in the 1931 CIE chromaticity diagram, as shown in Figure 10. The arrows indicate the changing trends of the color coordinates with increasing the

pump intensity. For the Yb,Tm,Ho:LTO, the color coordinates (x, y) have exhibited a change from (0.458, 0.388) to (0.261, 0.302) while the pump intensity increased from 4.1 to 79.0 W/cm^2. The color coordinates cross the whole white region which has indicated that the white light output can be modulated simply by adjusting the pump power. In particular, the color coordinates at the pump intensity of 18.1 W/cm^2 is calculated to be (0.329, 0.336). This is very close to the standard color coordinates (0.33, 0.33), suggesting that the Yb,Tm,Ho:LTO has a potential use in standard white light sources. The pump power tunable white upconversion emission were also studied in some other systems such as the Yb,Tm,Er and Yb,Tm,Ho tridoped $NaYF_4$[30], Yb,Tm,Er:SrY_2O_4[31], Yb,Tm,Er:Lu_2O_3[32], and Yb,Tm,Er:$LiNbO_3$[33]. Compared with the results of these studies the tuning range of the white light color coordinates for the Yb,Tm,Ho:LTO system is the broadest, which implies the Yb,Tm,Ho:LTO would have more potential advanced applications in the upconversion based optoelectronic device. It also should be noted that, the existence of energy transfer between the Tm^{3+} and Ho^{3+} ($^1G_4$+$^5I_8 \rightarrow {}^3H_6$ +$^5F_3$) will enhance the red emissions of Ho^{3+} ions. This would result the color coordinates of the Yb,Tm,Ho:LTO are more close to the red region compared with the Yb,Ho:LTO, especially at the condition of low pump intensity. With the increase of pump intensity, the color coordinates shifting towards to the blue region. This would be mainly ascribed to the fact that the blue emission intensity, which is nearly proportional to the third power of the pump intensity, grows much faster than the green and red emissions, both of which are nearly proportional to the second power of the pump intensity.

Conclusions

The rare earths of Yb^{3+}, Tm^{3+}, and Ho^{3+} doped LTO compounds were synthesized and the crystal structure parameters were obtained by a Rieveld refinement. The LTO crystal has a hexagonal structure with the space group P321. The rare earth Lu^{3+} occupies two lattice sites of 3e and 3f with the site symmetry of C_2 in this structure. Under the 976 nm laser excitation, the blue, green, and red UC emissions are generated from the $^1G_4 \rightarrow {}^3H_6$ (Tm^{3+}), $^5F_4$,$^5S_2 \rightarrow {}^5I_8$ (Ho^{3+}), and $^5F_5 \rightarrow {}^5I_8$ (Ho^{3+}) transitions, respectively. Based on the dependence of UC luminescence intensity on the pump power, the blue emission of the Tm^{3+} can be attributed to a three-phonon process while the green and red emissions were both attributed to a two-phonon process. The light color for the Yb,Tm,Ho:LTO were studied in the framework of 1931 CIE system. Result has suggested a strategy to fine-tune the UC emissions in a broad scope by simply controlling the pump power. This is different from that by precisely controlling the combinations of rare earth doping concentrations[34] or by changing the size of particles[35]. The desirable properties make the Yb,Tm,Ho:LTO promising in applications such as tunable solid-state light sources and UC based optoelectronic devices.

Acknowledgements

This work has been supported by the National Natural Science Foundation of China (grant 51302228), the Project for the Youth Talent of Chongqing (grant CSTC2014KJRC-QNRC0055), the Fundamental Research Funds for the Central Universities of Southwest University (grant XDJK2013C089 and XDJK2015B019) and the Doctoral Fund of Southwest University (Grant SWU114098).

References

1 H. A. Höppe, Angew. Chem. Int.Edit., 2009, 48, 3572-3582.
2 E. Downing, L. Hesselink, J. Ralston and R. Macfarlane, Science, 1996, 273, 1185-1189.
3 Z. Lu, J. Wang, X. Xiang, R. Li, Y. Qiao and C. M. Li, Chem. Commun., 2015, 51, 6373-6376.
4 F. Wang, D. Banerjee, Y. Liu, X. Chen and X. Liu, Analyst, 2010, 135, 1839-1854.
5 J. Zhou, Q. Liu, W. Feng, Y. Sun and F. Li, Chem. Rev., 2015, 115, 395-465.
6 I. Etchart, I. Hernandez, A. Huignard, M. Berard, W. P. Gillin, R. J. Curry and A. K. Cheetham, J. Mater. Chem., 2011, 21, 1387-1394.
7 J. H. Zeng, J. Su, Z. H. Li, R. X. Yan and Y. D. Li, Adv. Mater., 2005, 17, 2119-2123.
8 L. Xing, X. Wu, R. Wang, W. Xu and Y. Qian, Opt. Lett., 2012, 37, 3537-3539.
9 A. S. Gouveia-Neto, L. A. Bueno, R. F. do Nascimento, E. A. da Silva, E. B. da Costa and V. B. do Nascimento, Appl. Phys. Lett., 2007, 91, 091114.
10 L. W. Yang, H. L. Han, Y. Y. Zhang and J. X. Zhong, J. Phys. Chem. C, 2009, 113, 18995-18999.
11 G. S. Yi and G. M. Chow, J. Mater. Chem., 2005, 15, 4460-4464.
12 J.-C. Boyer, F. Vetrone, L. A. Cuccia and J. A. Capobianco, J. Am. Chem. Soc., 2006, 128, 7444-7445.
13 Q. Liu, Y. Sun, T. Yang, W. Feng, C. Li and F. Li, J. Am. Chem. Soc., 2011, 133, 17122-17125.
14 M. Haase and H. Schäfer, Angew. Chem. Int. Edit., 2011, 50, 5808-5829.
15 J. Llanos, R. Castillo, D. Barrionuevo, D. Espinoza and S. Conejeros, J. Alloy. Compd., 2009, 485, 565-568.
16 P. Höss and T. Schleid, Acta Crystallogr. E, 2007, 63, i133-i135.
17 S. F. Meier and T. Schleid, J. Solid. State. Chem., 2003, 171, 408-411.
18 J. Llanos and R. Castillo, J. Lumin., 2010, 130, 1124-1127.
19 J. Llanos, R. Castillo and W. Alvarez, J. Lumin., 2008, 62, 3597-3599.
20 S. Natansohn, J. Electrochem. Soc., 1969, 116, 1250-1254.
21 V. Petricek, M. Dusek, L. Palatinus, Jana2006, The Crystallographic Computing System, Institute of Physics: Praha, Czech Republic, 2006.
22 W. Pennington, J. Appl. Crystallogr., 1999, 32, 1028-1029.
23 J. Llanos, R. Castillo, D. Espinoza, R. Olivares and I. Brito, J. Alloy. Compd., 2011, 509, 5295-5299.
24 D. R. G. M. Pollnau, S. R. L üthi, H. U. G üdel, M. P. Hehlen, Phys. Rev. B, 2000, 61, 3337-3346.
25 G. Y. Chen, Y. Liu, Y. G. Zhang, G. Somesfalean, Z. G. Zhang, Q. Sun and F. P. Wang, Appl. Phys. Lett., 2007, 91, 133103.
26 Y. Kuisheng, L. Yan, Y. Chaoyi, L. Liping, Y. Chanhua and Z. Xiyan, J. Rare Earth, 2006, 24, 757-760.
27 C. Zhang, P. a. Ma, C. Li, G. Li, S. Huang, D. Yang, M. Shang, X. Kang and J. Lin, J. Mater. Chem., 2011, 21, 717-723.
28 J. Tang, C. Cheng, Y. Chen and Y. Huang, J. Alloy. Compd., 2014, 609, 268-273.

29 A. F. Henriques Librantz, S. D. Jackson, F. H. Jagosich, L. Gomes, G. Poirier, S. J. L. Ribeiro and Y. Messaddeq, J. Appl. Phys., 2007, 101, 123111.
30 J. J. Li, L. W. Yang, Y. Y. Zhang, J. X. Zhong, C. Q. Sun and P. K. Chu, Opt. Mater., 2011, 33, 882-887.
31 E. Pavitra, G. S. R. Raju, J.-H. Oh and J. S. Yu, New J. Chem., 2014, 38, 3413-3420.
32 Y. Li, J. Zhang, Y. Luo, X. Zhang, Z. Hao and X. Wang, J. Mater. Chem., 2011, 21, 2895-2900.
33 M. Marin-Dobrincic, J. A. Sanz-Garcia, E. Cantelar and F. Cusso, Mater. Lett., 2013, 96, 63-66.
34 F. Wang and X. Liu, J. Am. Chem. Soc., 2008, 130, 5642-5643.
35 S. Schietinger, L. D. Menezes, B. Lauritzen and O. Benson, Nano. Lett., 2009, 9, 2477-2481.

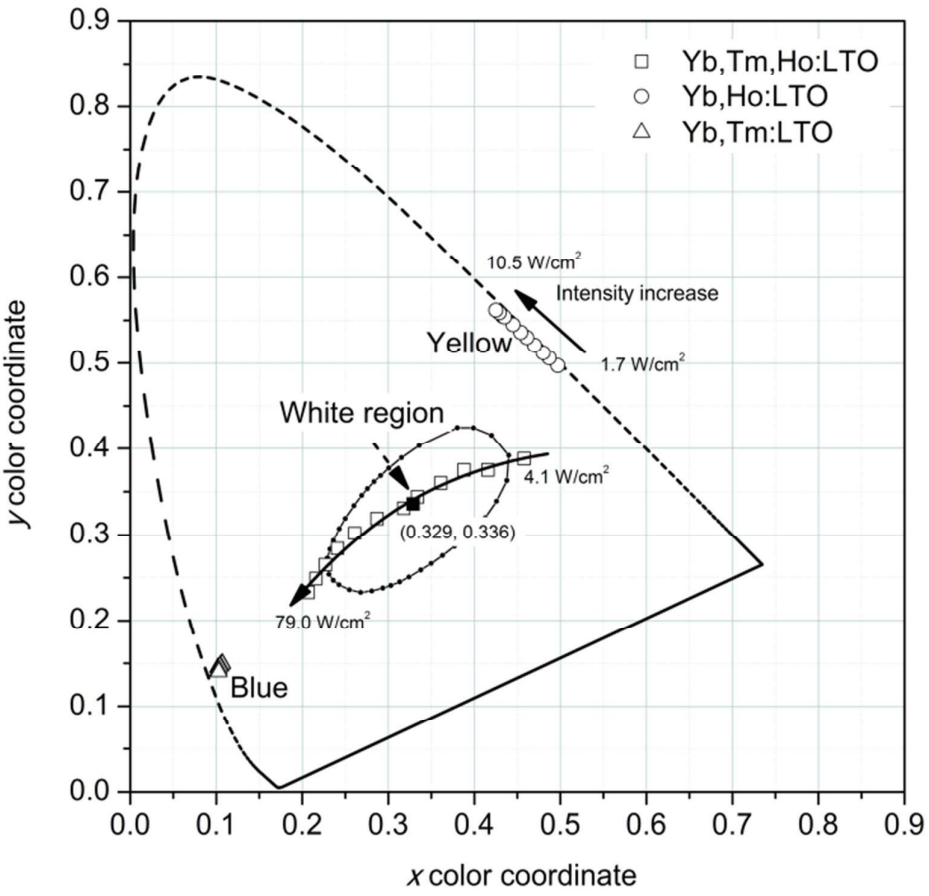

Tunable power driven white upconversion luminescence was realized in the Yb^{3+}, Tm^{3+}, and Ho^{3+} tri-doped Lu_2TeO_6.